

Analysis of the tilt and azimuth angles of photovoltaic systems in non-ideal positions for urban applications

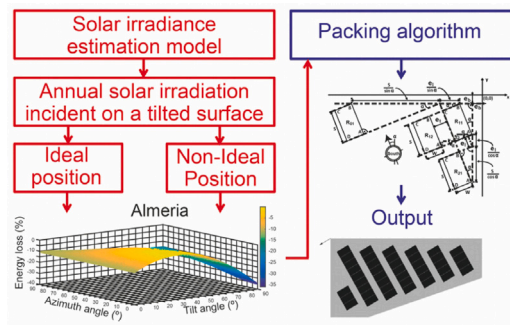
A. Barbón^a, C. Bayón-Cueli^c, L. Bayón^{b,*}, C. Rodríguez-Suanzes^c

^a Department of Electrical Engineering, University of Oviedo, Spain

^b Department of Mathematics, University of Oviedo, Spain

^c Polytechnic School of Engineering of Gijón, University of Oviedo, Spain

GRAPHICAL ABSTRACT



ARTICLE INFO

Keywords:

Photovoltaic systems
Tilt angle
Non-ideal position
Urban applications

ABSTRACT

A professional point of view suggests that photovoltaic systems should be installed at the optimum tilt angle and orientation. However, in photovoltaic systems integrated in buildings the flexibility of installation is common. This paper is organized in two different parts. In the first one, the energy losses caused by deviations from the tilt angle (β) and the orientation (γ) of the installation in relation to the ideal position are evaluated. This work considers the cloudy-sky conditions in each locality and theoretically calculates by applying the Cavalieri's principle, the energy losses. Ten cities around the world, in the northern hemisphere, have been studied with a MATLAB code and the findings demonstrate that non-ideal tilt and azimuth angles can also lead to acceptable levels of electric energy generation. A photovoltaic system installed in South orientation ($\gamma = 0^\circ$) and β deviations of up to 10° in relation to the optimum tilt angle has a very small influence on the energy losses. The energy losses are: 5%, 10%, 15% and 20% when β deviations are respectively: $21\text{--}23^\circ$, $31\text{--}33^\circ$, $37\text{--}40^\circ$ and $43\text{--}47^\circ$. Then, in the second part, an important application of this previous outcome comes out: the best distribution of the photovoltaic modules on a flat roof of irregular shape of an urban building is achieved. The aim of this work is to maximize the amount of energy get by a photovoltaic system. This engineering problem is highly complex as it involves 10 variables: the available flat roof area, the shape and the orientation of the available flat roof area, the dimensions (length and width) of the commercial photovoltaic modules, the orientation and the position of the photovoltaic modules, the number of the photovoltaic modules, the minimum distances (maintenance operations, to avoid shadowing effects) between rows of photovoltaic modules, and the minimum distance to the terrace boundary. In this context, this work aims to present a study to assist the decision-making.

This paper shows a packing algorithm (in Mathematica™) which maximizes the energy generation area of the solar photovoltaic system, considering shadings and distances required for maintenance. Eventually, using

* Corresponding author.

E-mail address: bayon@uniovi.es (L. Bayón).

the initial study, it comes out the influence of β on the potential capacity of the solar photovoltaic system and it is demonstrated that a decrease in the optimal tilt angle results in an increase up to 24% in the amount of obtained energy keeping invariable the available area. For example, in Almería, with an optimum tilt angle of 30.3 ($^{\circ}$) the amount of obtained energy is 149.8 (MWh) while with a tilt angle of 14 ($^{\circ}$) the amount of obtained energy is 186.2 (MWh). This analysis enables to find the optimal answer to the following practical questions: what number of photovoltaic modules is required?, which is the right position for the photovoltaic modules?, and what orientation of photovoltaic modules is the right one?. There are many installers of photovoltaic systems who would benefit from studies about this issue.

1. Introduction

Urban environments are considered to be important points for the installation of renewable energy technologies, due to their high density of energy consumption. By 2050, 66% of the world's population will be living in urban areas [1]. Among different types of available renewable energy technologies, the shown Solar Energy Systems (SESs) promise to be integrated applications for buildings. The SESs that can be used in the building sector are: solar thermal collectors, and photovoltaic (PV) systems. The solar thermal collectors that are used for heating and getting hot water, are: flat plate collectors and vacuum collectors. The installation of solar thermal collectors is more limited than that of PV systems, because it is accompanied by a water facility. However, the annual installed surface of flat plate collectors in the EU in 2017 has been of 1,802,194 (m^2), and that of vacuum collectors of 125,889 (m^2) [2]. With a power equivalent to 1372 (MWth).

In the case of PV systems, the features of their components allow a greater freedom of installation. Therefore, the global PV systems installations on rooftops are rapidly growing. Jacobson et al. [3] estimate that by 2050 the percentages of electricity generated by photovoltaic systems will be: residential roof PV (14.90%), commercial/government roof PV (11.60%), and solar PV plant (21.40%). The angles of a PV system that define its installation on rooftops are: the tilt and the azimuth angle. The tilt angle (β) is defined as the angle between the plane of the tilted surface and the horizontal plane ($\beta = 0^{\circ}$ in horizontal position of the surface, $\beta = 90^{\circ}$ in vertical position of the surface). The azimuth angle (γ) is defined as the angle between the projection on a horizontal plane of the normal to the tilted surface and South direction ($\gamma = -90^{\circ}$ in East, $\gamma = 0^{\circ}$ in South, $\gamma = 90^{\circ}$ in West).

The application of PV systems in buildings is classified into two categories: building-integrated photovoltaics (BIPV) and building-applied photovoltaics (BAPV). In a BIPV system, the PV module is fully integrated into the building frame as an additional building material. Different designs of building roofs for solar integration are shown in [4]. When the PV module is just located on the roof using additional mounting structure, the system is known as BAPV. If the roof is tilted, in BAPV and BIPV systems, the tilt angle of the PV modules depends on the roof slope of the structure. If the roof is flat, in BAPV systems, the tilt angle of the PV modules may be different from the roof slope of the structure, and the azimuth angle of the building should be considered when installing the PV modules.

The PV systems' installers in urban applications encounter some difficulties in getting the optimum angles in practical applications. There are several factors which require flexibility in the installation of PV systems:

(i) Aesthetic factor. This aspect is related to the architectural visual effect of the building. It is not enough for a PV to be functional, the point of view of its shape also is mandatory to be considered [5]. The environmental impact related to the aesthetic perception of PV systems implementation has been studied by several authors due to its relevance [6–8]. Therefore, it is necessary to reach good compromises between shape and function, where performances for an acceptable generation of electric energy and a pleasant architectural integration can coexist.

(ii) Available roof area factor. The available roof area is the area that can be used for installing PV systems. In order to calculate

the available roof area, various building components must be taken into account, such as: chimneys, elevator machine rooms, fans, and plumbing vents [9].

(iii) Shading factor. Shadings from nearby buildings, of the roof itself and of building components are very important factors that decrease the power output of PV systems. A 3D city model would be necessary to precisely determine this factor [10].

(iv) PV modules separation factor. Numerous legislations require a minimal separation between rows of PV modules to minimize the row to row shading. For example, the Spanish Government Technical Report [11] states that, in order to minimize shading effects, the distance between row to row of PV modules has to guarantee a minimum of 4 (h) of sunshine around noon on the winter solstice. Therefore, no separation is necessary to avoid row to row shading.

(v) Service area factor. The service area is the necessary space for maintenance operations. This factor depends on the PV modules' separation factor. If tilt angle is high, the space freed up due to the spacing between the rows of PV modules can be used for this function [12]. Table 9 presented by Byrne et al. [12] relates the tilt angle to the service area.

(vi) Dust deposition factor. Dust accumulation is one of the most important factors that affect the PV modules efficiency [13]. In those regions frequently affected by sand storms this is a critical factor. Air pollution also affects the choice of the optimum angles. Dust deposition is a function of numerous factors. Grupta et al. [14] list the most important factors. This work focuses on tilt and azimuth angles. The tilt angle is a major factor which affects the dust deposition process [14].

As the Sun's position changes throughout the day, the solar tracker is the most efficient method of increasing the energy on tilted surfaces. A two-axis tracking is able to accurately follow the Sun's path in the daytime. It is obvious that the incident solar irradiance in PV modules with single-axis tracking or two-axis tracking exceeds that of PV modules with a fixed tilt angle all through the year. Dual-axis tracker systems increase the total energy production by 18%–29% compared to fixed-tilt systems [15] and single-axis tracker systems increase total energy production by 15%–24% compared to fixed-tilt systems [15,16]. These results depend on the geographical location of each particular site. However, solar tracking systems are quite expensive, they consume electrical energy and they also have a maintenance cost. Dual-axis tracker systems generally add a premium of 40–50% to the overall system costs when compared to fixed-tilt systems of a similar size [16,17]. And single-axis tracker systems generally add a premium of 20–25% to the overall system costs when compared to fixed-tilt systems of a similar size [16,17]. This high relative cost of driving reduces the economic effect of solar tracking systems so that they are not recommended to be used in PV modules in the building sector [18,19]. The use of the annual optimum tilt angle can be a good option as an alternative.

There are applications in the building sector that require the use of simple methods to determine the tilt and azimuth angles. It has been widely acknowledged that the optimum azimuth angle for tilted surfaces is facing due South, in the northern hemisphere (In the southern hemisphere, it is facing due North) [20]. If the roof is tilted, in BAPV and BIPV systems, usually, its orientation is not exactly faced to the South. The choice of the optimum tilt angle is a more complicated issue, because it depends on several factors [21] such as latitude

Nomenclature

A_{PV}	Total photovoltaic modules area (m ²)
A_{PV}^{β}	Total photovoltaic modules area for fixed tilt (m ²)
<i>Energy loss</i>	Energy loss (%)
e_b	Terrace boundary distances (m)
e_l	Longitudinal distance (m)
e_l^m	Longitudinal maintenance distance (m)
e_l^{st}	Longitudinal standard distance (m)
e_t	Transversal maintenance distance (m)
\mathbb{H}_t	Adjusted total irradiation on a tilted surface (Wh/m ²)
\mathbb{H}_t^{β}	Adjusted annual total irradiation for fixed tilt (Wh/m ²)
\mathbb{H}_t^a	Adjusted annual total irradiation (Wh/m ²)
L	Length of the photovoltaic modules (m)
\mathbb{I}_{bh}	Adjusted beam irradiance on a horizontal surface (W/m ²)
\mathbb{I}_{bt}	Adjusted beam irradiance on a tilted surface (W/m ²)
\mathbb{I}_{dh}	Adjusted diffuse irradiance on a horizontal surface (W/m ²)
\mathbb{I}_{dt}	Adjusted diffuse irradiance on a tilted surface (W/m ²)
\mathbb{I}_{rt}	Adjusted ground reflected irradiance on a tilted surface (W/m ²)
\mathbb{I}_t	Adjusted total irradiance on a tilted surface (W/m ²)
n	Ordinal of the day (day)
N	Number of photovoltaic modules
S	Projection the L on the horizontal plane (m)
T	Solar time (h)
T_R	Sunrise solar time (h)
T_S	Sunset solar time (h)
W	Width of the photovoltaic modules (m)
α	Angle that the terrace forms with the N–S direction (°)
α_S	Height angle of the Sun (°)
β	Tilt angle of photovoltaic module (°)
β^*	Tilt angle of photovoltaic module for the maximization of the total energy (°)
β_{opt}	Optimal annual tilt angle (°)
γ	Azimuth angle of photovoltaic module (°)
γ_{opt}	Optimal annual azimuth angle (°)
γ_S	Azimuth of the Sun (°)
δ	Solar declination (°)
θ_i	Incidence angle (°)
θ_{i0}	Longitudinal incidence angle that minimizes shadowing effects (°)
θ_z	Zenith angle of the Sun (°)
λ	Latitude angle (°)
ρ_g	Ground reflectance (dimensionless)
ω	Hour angle (°)

of the location, climate condition, distribution of beam and diffuse solar irradiance and air pollution. Therefore, the tilt angle is a critical parameter for installing fixed-tilt *PV* modules. For this choice there have been proposed several very diverse options.

Table 1

Correlations between the annual optimum tilt angle and latitude.

Author	Recommended annual tilt angle
Duffie & Beckmann [20]	$(\lambda + 15^\circ) \pm 15^{\circ a}$
Heywood [25]	$\lambda - 10^\circ$
Lunde [26]	$\lambda \pm 15^{\circ a}$
Chinnery [27]	$\lambda + 10^\circ$
Luque et al. [28]	$3.7 + 0.69 \cdot \lambda $
Chang [29]	$\begin{cases} 2.14 + 0.764 \cdot \lambda & \text{if } \lambda \leq 65^\circ \\ 33.65 + 0.224 \cdot \lambda & \text{if } \lambda > 65^\circ \end{cases}$
Talebizadeh et al. [30]	$7.203 + 0.6804 \cdot \lambda$
Jacobson et al. [31]	$1.3793 + 1.2011\lambda - 0.014404\lambda^2 + 0.000080509\lambda^3$

^aThe minus (plus) sign refers to the summer (winter) season.

Numerous models provide estimates of optimal tilt angles obtained from different methods at different sites around the world [22]. These models differ between them in simplicity, use and accuracy. Their complexity increases with their accuracy. These models can be separated into two categories: calculations that use the latitude angle and calculations that maximize the total solar irradiance which comes down onto the tilted surface. The first methods are simple but they are approximate. The second ones are more accurate but they have a strong dependence on the model of solar irradiance and their use is more complex.

Many authors have calculated the optimal tilt angle for a given location. But the result they have obtained is not suitable for other locations [23]. Therefore, the installers of solar energy system need simple tilt angle-latitude relationships to be used as the rule of thumb. The simplicity of use and the accuracy are the most important features. A brief review of the various simple relationships is summarized in Table 1. A full review is shown by [24].

As a consequence of this, numerous models provide estimates of the optimum angles in solar energy applications obtained from different methods at different sites around the world. However, there is little information on the assessment of the energy received by *PV* systems for any orientation and any tilt angles that deviate from the ideal ones. For example, Chen et al. [32] demonstrate that a quite large range of installation angles of *PV* systems annually causes negligible energy losses. Al Garni et al. [33] present a model to analyse the tilt angles between 0 (°) and 90 (°) in one-degree steps to find out the annual solar irradiation that reaches a tilted surface, in order to calculate the optimum tilt angle. Sánchez et al. [34] present an experimental study which shows that small deviations from the optimum tilt angle do not cause great energy losses.

This work is divided into two different parts. The first, one explores the potential energy of solar energy systems in non-ideal positions for urban applications. In the second part, with the help of the previous study, a practical application is presented. The specific contributions of this study can be summarized in the following proposals:

- (i) A mathematical method to calculate the optimum tilt angle by the application of the Cavalieri's principle.
- (ii) A detailed analysis of the energy losses in function of the tilt and the azimuth angles of solar energy systems in non-ideal positions for urban applications.
- (iii) A method to compute the optimum distribution of *PV* modules on a flat roof of an urban building.

With regard to bullet (i), this is the first time the Cavalieri's principle has been used for maximizing the solar irradiance in *PV* modules.

In the bullet (ii), the meteorological conditions in each particular site are taken into account using an approaching technique based on the use of Fourier series to incorporate cloudy-sky models. As discussed in the practical application of this study, it is necessary to know how the tilt and azimuth angles of the *PV* module affect the amount of solar energy collected on tilted surfaces under non-ideal positions. Therefore,

one of the objectives of this study is to demonstrate that for some tilt angles, they cause negligible annual energy losses. The calculations have shown that the installation of *PV* modules with $\gamma = 0$ ($^{\circ}$) and tilt angle deviations of up to 10 ($^{\circ}$) in relation to the optimum tilt angle has a very little influence on the incoming solar irradiation of up to 1%.

In the bullet (iii), in relation to the classical packing mathematical problem, a practical application is presented. The algorithm is based on previous studies [35], where a two-dimensional rectangle packing problem and Linear Fresnel Reflectors (*LFRs*) have been considered. This study contemplates terraces with irregular shapes and it uses *PV* modules in which their tilt angle, β , will play an important role, instead of *LFRs*. So far, this particular issue has not been addressed in the literature. The algorithm, for each tilt angle β , maximizes the total area of the *PV* modules, taking into account the available area and the physical restrictions. It is obvious that, for the β_{opt} the solar irradiance captured by each *PV* module will be the greatest one. But if the shading between the rows of *PV* modules, and the option of positioning the *PV* modules out of its β_{opt} are taking into account a greater area of *PV* modules can be get by reducing the irradiance captured by each one. Along the first part of this study the quantity of this irradiance for a non ideal positioning is obtained. The concluding solution will find a tilt angle β value, so that the total amount of energy captured by all the *PV* modules on the roof will be maximized.

Installers of solar energy systems think that *PV* modules should only be installed on surfaces with ideal tilt and azimuth angles and this is a false perception [36]. However, this engineering problem is highly complex as it involves 10 different variables: the available flat roof area, the shape and the orientation of the available flat roof area, the dimensions (length and width) of the commercial *PV* modules, the orientation and the position of the *PV* modules, the number of the *PV* modules, the minimum distances (maintenance operations, to avoid shadowing effects) between rows of *PV* modules, and the minimum distance to the terrace boundary. In this context, this work aims to present a study to assist the decision-making. These analyses enable to find the optimal answer to the following practical questions: what number of *PV* modules is required?, which is the right position for

PV modules?, and what orientation of *PV* modules is the right one?. There are many installers of *PV* systems who would benefit from studies about this issue.

This paper is organized with the following structure: The governing equations and the optimization method are presented in Section 2. The application to solve the problem of an optimum distribution of *PV* modules on the roofs is outlined in Section 3. Geographic characteristics of the cities under study, numerical simulations for different tilt and azimuth angles and findings on the influence of a non ideal positioning on the distribution of *PV* modules are presented in Section 4. Finally, Section 5 summarizes the main contributions and the conclusions of the paper.

2. Background and optimization method

The work described in this section was carried out in four steps:

(i) Analysis of the most suitable solar irradiance estimation models for the study, because, the accuracy to determine the ideal position of a *PV* system depends on the availability of solar irradiance data.

(ii) Determination of the annual solar irradiation incident on a tilted surface. For this purpose, an analysis of the models used to determine the three components of solar irradiance (beam, diffuse and ground reflected) on a tilted surface is carried out.

(iii) Determination of the optimum tilt angle. It is also necessary to use a method to maximize the amount of solar irradiance that gets the surface of the *PV* module. For this purpose, the Cavalieri's principle of integral calculus is used.

(iv) Evaluation of the non-ideal position of a *PV* system in terms of energy performance.

This study assumes the following points:

- (i) The weather conditions of each particular site are considered.
- (ii) The isotropic model of Liu and Jordan [37] to calculate the diffuse solar irradiance on a tilted surface is used.
- (iii) The annual ideal position of the *PV* modules is considered.

2.1. Solar irradiance estimation model

The distribution of annual solar irradiance is specific for each particular site, with remarkable variations produced by the distribution of the local cloudy cover. Therefore, the ideal positioning (optimal tilt and azimuth angles) of the *PV* module is specific for each particular site. In order to estimate the annual solar irradiance on tilted surfaces in ideal or non-ideal positions, a set of precise data about the solar irradiance received by the Earth for the studied geographical location is needed. The most common available data in ground-level meteorological stations refers to global and diffuse solar irradiance on horizontal surfaces. In the absence of meteorological data from ground-level meteorological stations, the methods to determine the optimum tilt angle are just an approach to the accurate models for the estimation of solar irradiance in a given site, therefore, they are only approximate.

In technical literature, different models to estimate each component of the solar irradiance have been published. The accuracy of these models is different in different latitudes [38]. There are many different models such as the clear-sky models [39], the satellite based models [40], the temperature based methods [41], etc.

In the present paper, the method presented by [42] has been used to determine the adjusted hourly beam and diffuse solar irradiance on a horizontal surface to the weather conditions of a particular site and for each day of the year. This method is based on the Hottel's model [43] to estimate the beam solar irradiance transmitted through clear atmosphere, the Liu's and Jordan's model [44] has been used to determine diffuse solar irradiance through a clear-sky, and the Fourier series approximation have been used to correct the clear-sky models and to adapt them to the climatological conditions of a specific location. In this way, with the theoretical solar irradiance on a tilted surface I_t , the adjusted irradiance has been calculated, I_t' . This method demonstrates its accuracy and its application to different climates compared with the actual data obtained from ground-level stations (*WRDC* database [45]). For example, in Wien (Austria), city under study in this paper, the R^2 value for daily beam irradiation is 0.85713 and the R^2 value for daily diffuse irradiation is 0.948112. These values are generally considered proof of a very good fit [46]. Several studies have already applied this procedure [47–49].

2.2. Annual solar irradiation incident on a tilted surface

Eq. (1) shows the adjusted total solar irradiation on a tilted surface, $\mathbb{H}_t(n, \beta, \gamma)$, for each day of the year, n , different values of tilt angle, β , and different values of azimuth angle, γ . This equation is adjusted to each location and to each type of climate, therefore, is adjusted under real weather conditions [20]:

$$\mathbb{H}_t(n, \beta, \gamma) = \int_{T_R(n)}^{T_S(n)} \mathbb{I}_t(n, T, \beta, \gamma) dT \quad (1)$$

where $\mathbb{I}_t(n, T, \beta, \gamma)$ (W/m^2) is the adjusted hourly distribution of total solar irradiance on a tilted surface, T_R (h) is the sunrise solar time, and T_S (h) is the sunset solar time.

The adjusted hourly distribution of total solar irradiance on a tilted surface, $\mathbb{I}_t(n, T, \beta, \gamma)$, is decomposed into three components: beam solar irradiance, diffuse solar irradiance, and ground reflected solar irradiance. The beam solar irradiance is the part of total solar irradiance which is received from the sun without atmospheric scattering [20]. The diffuse solar irradiance is the part of total solar irradiance which is received from the Sun when its direction has been changed by atmospheric scattering [20]. The ground reflected solar irradiance is a fraction of the total solar irradiance which is reflected by the surface

of the earth and by any other surface (buildings, trees, ...). Therefore, $\mathbb{I}_t(n, T, \beta, \gamma)$ can be calculated [20]:

$$\mathbb{I}_t(n, T, \beta, \gamma) = \mathbb{I}_{bt}(n, T, \beta, \gamma) + \mathbb{I}_{dt}(n, T, \beta) + \mathbb{I}_{rt}(n, T, \beta) \quad (2)$$

where $\mathbb{I}_t(n, T, \beta, \gamma)$ (W/m^2) is the adjusted hourly distribution of total solar irradiance on a tilted surface, $\mathbb{I}_{bt}(n, T, \beta, \gamma)$ (W/m^2) is the adjusted hourly distribution of beam solar irradiance on a tilted surface, $\mathbb{I}_{dt}(n, T, \beta)$ (W/m^2) is the adjusted hourly distribution of diffuse solar irradiance on a tilted surface, and $\mathbb{I}_{rt}(n, T, \beta)$ (W/m^2) is the adjusted hourly distribution of ground reflected solar irradiance on a tilted surface.

The adjusted hourly distribution of beam solar irradiance on a tilted surface can be calculated by the geometrical relationship between horizontal and tilted surfaces [20]:

$$\mathbb{I}_{bt}(n, T, \beta, \gamma) = \mathbb{I}_{bh}(n, T) \cdot \frac{\cos \theta_i}{\cos \theta_z} \quad (3)$$

where $\mathbb{I}_{bh}(n, T)$ (W/m^2) is the adjusted hourly distribution of beam solar irradiance on a horizontal surface, θ_z (rad) is the zenith angle of the Sun, θ_i (rad) is the incident angle. The adjusted hourly distribution of beam solar irradiance on a horizontal surface has been calculated using the method proposed by [42]. The incident angle θ_i (rad) on a tilted surface can be determined according to [20]:

$$\begin{aligned} \cos \theta_i = & \sin \delta \cdot \sin \lambda \cdot \cos \beta - \sin \delta \cdot \cos \lambda \cdot \sin \beta \cdot \cos \gamma + \cos \delta \cdot \cos \lambda \cdot \cos \beta \cdot \cos \omega \\ & + \cos \delta \cdot \sin \lambda \cdot \sin \beta \cdot \cos \gamma \cdot \cos \omega + \cos \delta \cdot \sin \beta \cdot \sin \gamma \cdot \sin \omega \end{aligned} \quad (4)$$

where δ (rad) is the solar declination, λ (rad) is the latitude, β (rad) is the tilt angle, γ (rad) is the azimuth angle and ω (rad) is the hour angle. When the (4) is used, it is necessary to ensure that: (i) the incident angle may exceed 90° , which means that the Sun is behind the surface; and, (ii) the Earth is not blocking the Sun.

The adjusted hourly distribution of diffuse solar irradiance on a tilted surface can be calculated [37]:

$$\mathbb{I}_{dt}(n, T, \beta) = \mathbb{I}_{dh}(n, T) \cdot \left(\frac{1 + \cos \beta}{2} \right) \quad (5)$$

where $\mathbb{I}_{dh}(n, T)$ (W/m^2) is the adjusted hourly distribution of the diffuse horizontal solar irradiance, and β (rad) is the tilt angle. Eq. (5) uses the isotropic model of Liu and Jordan [37] to calculate the diffuse solar irradiance on a tilted surface. The Liu and Jordan model [37] is commonly recommended for predicting diffuse solar irradiance at locations across the world [20,50,51]. The adjusted hourly distribution of the diffuse horizontal solar irradiance has been calculated using the method proposed by [42].

The adjusted hourly distribution of ground reflected solar irradiance on a tilted surface can be calculated [37]:

$$\mathbb{I}_{rt}(n, T, \beta) = (\mathbb{I}_{bh}(n, T) + \mathbb{I}_{dh}(n, T)) \cdot \rho_g \cdot \left(\frac{1 - \cos \beta}{2} \right) \quad (6)$$

where $\mathbb{I}_{bh}(n, T)$ (W/m^2) is the adjusted hourly distribution of beam solar irradiance on a horizontal surface, $\mathbb{I}_{dh}(n, T)$ (W/m^2) is the adjusted hourly distribution of diffuse solar irradiance on a horizontal surface, β (rad) is the tilt angle, and ρ_g is the ground reflectance (dimensionless). The adjusted hourly distribution of the ground reflected solar irradiance on a tilted surface has been determined with the model of Liu and Jordan [37].

In order to show the application of the above equations, Cairo (Egypt) (Latitude: $30^\circ 29' 24''\text{N}$, Longitude: $31^\circ 14' 38''\text{W}$, Altitude: 41 (m)), has been selected between the ten chosen cities for this work. Fig. 1 shows the adjusted total solar irradiation on a tilted surface $\mathbb{H}_t(n, \beta, 0)$ for different values of tilt angle, β , and $\gamma = 0^\circ$. Fig. 2 shows the adjusted total solar irradiation on a tilted surface $\mathbb{H}_t(n, 24.2, \gamma)$ for different values of azimuth angle, γ , and $\beta = 24.2^\circ$ (this is, as it will be shown later, its value β_{opt} in Cairo).

Eq. (7) shows the adjusted annual solar irradiation on a tilted surface, $\mathbb{H}_t^a(\beta, \gamma)$, for different values of tilt angle, β , and different

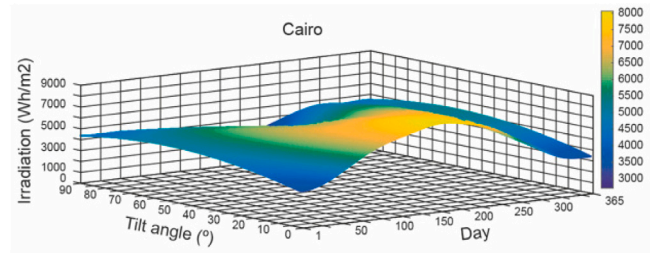


Fig. 1. Adjusted total solar irradiation on a tilted surface $\mathbb{H}_t(n, \beta, 0)$.

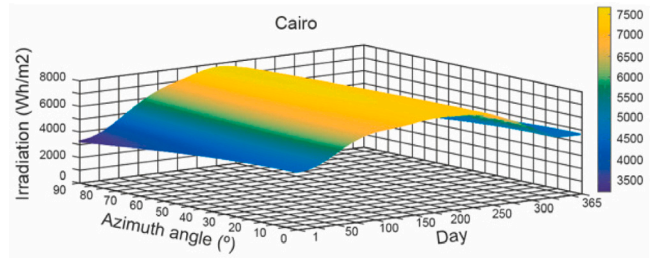


Fig. 2. Adjusted solar irradiation on a tilted surface $\mathbb{H}_t(n, 24.2^\circ, \gamma)$.

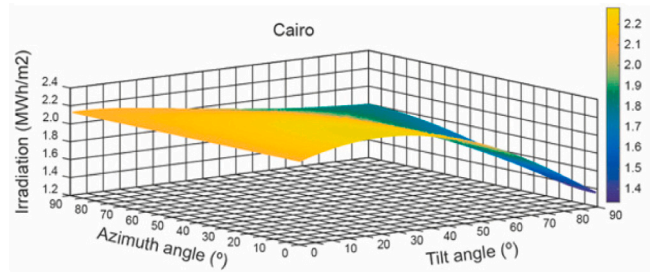


Fig. 3. Adjusted annual solar irradiation on a tilted surface $\mathbb{H}_t^a(\beta, \gamma)$.

values of azimuth angle, γ :

$$\mathbb{H}_t^a(\beta, \gamma) = \sum_{n=1}^{365} \mathbb{H}_t(n, \beta, \gamma) \quad (7)$$

Fig. 3 shows the adjusted annual solar irradiation on a tilted surface $\mathbb{H}_t^a(\beta, \gamma)$ in Cairo.

2.3. Ideal position

The tilt and the azimuth position of the PV module both affect the amount of solar irradiance that hits the PV module surface. The ideal position is defined by the optimum tilt angle (β_{opt}) and the optimum azimuth angle, which, as it is well known is $\gamma_{opt} = 0^\circ$ in the northern hemisphere [21,22]. The ideal position can be referred to a year, a month, a day or an hour and this annual ideal position has been considered.

An approach to choosing the ideal position of a PV module is to maximize the amount of total irradiance falling onto its surface. These methods offer good results in sunny climates where the beam radiation component dominates. In cloudiest climates, the diffuse radiation component increases its importance. In these cases, it is essential to take into account the frequency and intensity of cloud cover using an appropriate model to estimate the solar irradiance. This model also takes into account the effect of the weather conditions.

A methodology based on maximizing the total irradiation which comes down onto the tilted surface has been used to determine the annual ideal position. This methodology takes into account the effect of

the weather conditions. The volume underneath the graph (see Fig. 1) of the two-variable function, $\mathbb{H}_t(n, \beta, 0)$, is given by the double integral:

$$\iint_D \mathbb{H}_t(n, \beta, 0) \, dnd\beta \quad (8)$$

where D is the rectangle $D : [1, 365] \times [0, 90]$. The optimization procedure is in fact the application of Cavalieri's principle of integral calculus, whose proper generalization is Fubini's Theorem [52]. In order to compute β_{opt} , an interval $[0, 90]$ has been taken and the integral for each one of the values provided in this interval has been computed. Following the Cavalieri idea, it has been computed the integral:

$$\mathbb{H}_t^\beta(\beta) = \int_1^{365} \mathbb{H}_t(n, \beta, 0) \, dn \quad (9)$$

where, for convenience, the value $\gamma = 0$ has been removed from the nomenclature. In the end, the value of β which arises, shows:

$$\max_{\beta} \mathbb{H}_t^\beta(\beta) \quad (10)$$

Then, this optimum tilt angle, β_{opt} , has been denoted and this curve $H_t^\beta(\beta)$ has been used later on in the application to distribute the PV modules on flat roofs.

2.4. Non-ideal position: Energy loss

From the point of view of non-ideal position, a PV system can be evaluated in terms of energy performance. This study evaluates energy losses produced by deviations from the tilt and azimuth angle of the installation (non-ideal position) compared to those of the optimal angles (ideal position). With this purpose, the difference between the annual energy absorbed in a non-ideal position ($\mathbb{H}_t^a(\beta, \gamma)$) and that absorbed in an ideal position ($\mathbb{H}_t^a(\beta_{opt}, \gamma_{opt})$) have been computed. These values are % of the energy loss, related to the ideal position, that is:

$$Energy \, loss = \frac{\mathbb{H}_t^a(\beta, \gamma) - \mathbb{H}_t^a(\beta_{opt}, \gamma_{opt})}{\mathbb{H}_t^a(\beta_{opt}, \gamma_{opt})} \times 100 \quad (11)$$

3. Distribution of PV modules on flat roofs

This paper proposes a new methodology to determinate the optimum distribution of PV modules on a flat roof of an urban building. The methodology includes four steps to identify the required number of PV modules, their position and their orientation to maximize the total energy absorbed by them. A flowchart outlining the proposed methodology is shown in Fig. 4.

The first step of the methodology describes the optimization mathematical problem which aims for maximizing the total PV modules area (A_{PV}). In addition, in this step the parameters of the PV module are defined. The second step of the procedure consists of a study of the shadings produced between the rows of PV modules. The third step searches for the packing algorithms that maximize the total PV modules area. The fourth step of the procedure is the choice of the tilt angle of the PV modules to maximize the total energy produced by the PV system.

The following considerations have been made in this study:

- (i) The shape of the available roof area is irregular.
- (ii) The available roof area can have any orientation.
- (iii) The dimensions (length and width) of the commercial PV module are invariable.
- (iv) The minimum distances between rows of PV modules are taken into account in order to allow maintenance and to avoid shading effects.

The number, the position, and the orientation of the PV modules are outputs of the algorithm.

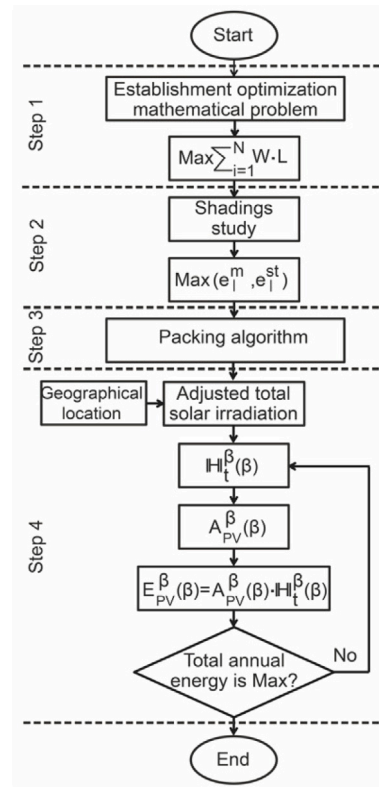


Fig. 4. A flowchart outlining the proposed methodology.

3.1. Area maximization and shadows study

This first subsection describes the optimization mathematical problem which aims for maximizing the total PV modules area (A_{PV}), given by:

$$A_{PV} = \sum_{i=1}^N W \cdot L \quad (12)$$

where N is the number of PV modules, W is the width of a PV module, and L is the length of a PV module. Only one type of commercial PV module has been used in the study. Referring to restrictions, the model first has considered a transversal installation distance (e_t) to get an accurate installation of PV modules. Secondly a longitudinal maintenance distance (e_l^m) between the rows of PV modules in order to allow a proper inspection, cleaning, and maintenance has been considered. A minimum distance between the roof boundary and the PV modules (e_b), for maintenance purposes has also been kept.

Eventually, the shadings produced in between the rows of PV modules are an essential aspect that has to be considered. Fig. 5 shows a row of South-orientated PV modules ($\gamma_{opt} = 0^\circ$).

It can be easily deduced that for the longitudinal component it comes true:

$$\tan \theta_l = \frac{\cos \alpha_s \cos \gamma_s}{\sin \alpha_s} = \frac{\cos \gamma_s}{\tan \alpha_s} = \tan \theta_z \cos \gamma_s \quad (13)$$

where α_s is the height angle of the Sun ($^\circ$), θ_z is the zenith angle of the Sun ($^\circ$) and γ_s is the azimuth of the Sun ($^\circ$).

The Spanish Government Technical Report [11] states that, in order to minimize shading effects, the distance between reflectors has to guarantee a minimum of 4 hours of sunshine around noon on the winter solstice. Here the longitudinal incidence angle that minimizes shading effects (13) on December 21 at 10 : 00 is named θ_{l0} . From Fig. 6 it is immediately obtained that the longitudinal distance, according to the previous standard (e_l^{st}), in order to avoid the shadings in between two

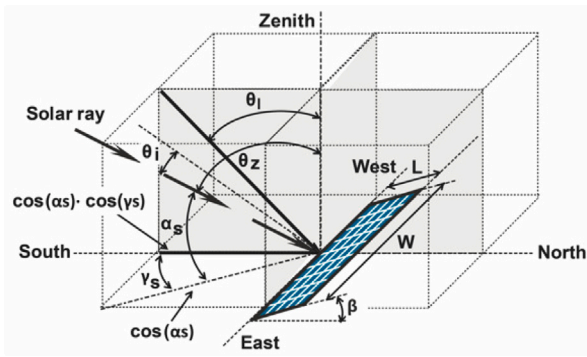


Fig. 5. Longitudinal and transversal study of the installation.

consecutive rows of PV modules, is:

$$e_l^{st} = S \frac{\tan \beta_{opt}}{\cot \theta_{l0}} = L \frac{\sin \beta_{opt}}{\cot \theta_{l0}} \quad (14)$$

where $S = L \cos \beta_{opt}$ is the projection of the length of the PV module on the horizontal plane. The definitive value that is imposed as the longitudinal distance (e_l) is:

$$e_l = \max[e_l^m, e_l^{st}] \quad (15)$$

So that not only a distance that allows the maintenance of the PV system but also the fulfilment of the standard itself are guaranteed.

It is very important to highlight, as it is shown later on in Section 4.4, that the fulfilment of the standard (14) will ensure an almost total absence of shading in between the rows of PV modules during the valid operation time of the PV module all through the year.

3.2. Packing algorithm

Here the algorithm presented in [35] has been generalized, using PV modules instead of Linear Fresnel Reflectors and considering terraces with an arbitrary shape instead of a rectangular shape. The packing scheme consists of placing rows of PV modules to the East–West direction, South-orientated with dimensions $W \times L$. Therefore, the projection on the horizontal plane of a PV module with dimensions $W \times S$ has been considered. Identical rectangles have been packed in a fixed region taking into account two constraints: (i) A minimum space between objects for installation, maintenance and to avoid shading effects; (ii) The orientation of the objects is fixed in relation to the Sun. So far, this packing problem has not been addressed in the literature.

Given a roof of fixed dimensions, the packing starts in one of the corners of the roof with a right angle. In Fig. 7, maintaining the generalization – just in this case –, this is the upper-right corner. If the terrace has not any corner with a right angle, the procedure will be also valid by inscribing the terrace shape inside a rectangle. Then taking the roof edges in this corner parallel to the reference axes ($x-y$)

and being α the angle between the N–S direction and the positive axis y , a base rectangle R_{11} is defined using two vertices A y B , which are located as close as possible to the upper-right corner of the roof (see Fig. 7).

The coordinates of the two basic vertices $A(x_A, y_A)$, $B(x_B, y_B)$, are given by:

$$R_{11} : \begin{cases} A(e_b, e_b + S \cos \alpha) \rightarrow D(x_A + W \cos \alpha, y_A + W \sin \alpha) \\ B(e_b + S \sin \alpha, e_b) \rightarrow C(x_B + W \cos \alpha, y_B + W \sin \alpha) \end{cases} \quad (16)$$

As it is shown, once A and B have been calculated, the other two vertices C and D will be immediately obtained. This procedure has been repeated with the same formulae in all the cases that have been studied.

Firstly, the packing pattern places in a vertical order, from top to bottom, as many rectangles R_{1i} as possible:

$$R_{1i} : \begin{cases} A(x_A, y_A + (i - 1)\Delta y) \rightarrow D \\ B(x_B, y_B + (i - 1)\Delta y) \rightarrow C \end{cases} \quad (17)$$

with:

$$\Delta x = 0; \Delta y = \begin{cases} \frac{e_l}{\cos \alpha} + \frac{S}{\cos \alpha} & \text{if } \alpha \neq \pi/2 \\ e_l + W & \text{if } \alpha = \pi/2 \end{cases} \quad (18)$$

From each rectangle in this first column R_{1i} , new rectangles R_{ij} (with $j = 1, \dots, m$) are added in W–E direction:

$$R_{ij} : \begin{cases} A(x_A + (j - 1)\delta x, y_A + (j - 1)\delta y) \rightarrow D \\ B(x_B + (j - 1)\delta x, y_B + (j - 1)\delta y) \rightarrow C \end{cases} \quad (19)$$

with:

$$\delta x = \begin{cases} e_l \cos \alpha + W \cos \alpha & \alpha \neq \pi/2 \\ e_l \sin \alpha + S \sin \alpha & \alpha = \pi/2 \end{cases} \quad (20)$$

$$\delta y = \begin{cases} e_l \sin \alpha + W \sin \alpha & \alpha \neq \pi/2 \\ 0 & \alpha = \pi/2 \end{cases} \quad (21)$$

Finally, the packing pattern is completed placing new rectangles R_{k1} ($k = 0, -1, \dots$) horizontally aligned with the base rectangle R_{11} :

$$R_{k1} : \begin{cases} A(x_A + (1 - k)\Delta x, y_A) \rightarrow D \\ B(x_B + (1 - k)\Delta x, y_B) \rightarrow C \end{cases} \quad (22)$$

with:

$$\Delta x = \begin{cases} \frac{e_l}{\sin \alpha} + \frac{S}{\sin \alpha} & \text{if } \alpha \neq 0 \\ e_l + W & \text{if } \alpha = 0 \end{cases}; \Delta y = 0 \quad (23)$$

3.3. Maximization of the total energy

Eventually, after all the issues previously exposed, the method that is proposed to maximize the total energy produced by the PV system consists in:

- (1) Calculating the irradiance curve as a function of the tilt:

$$\mathbb{H}_t^{\beta}(\beta) \quad (24)$$

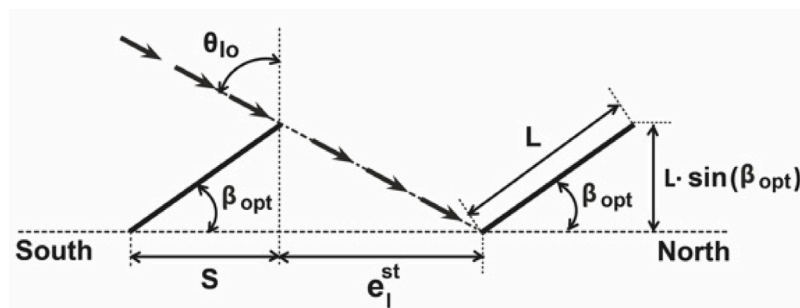


Fig. 6. Longitudinal study of shadows.

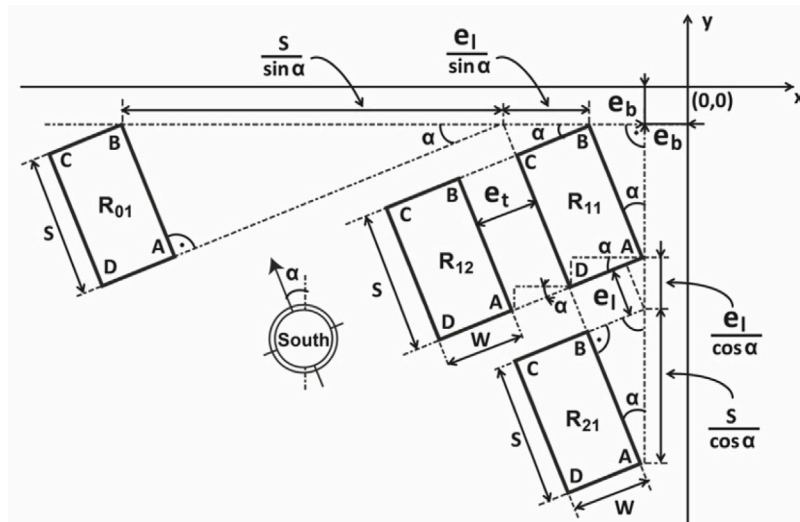


Fig. 7. Packing algorithm.

(2) Carrying out the packing algorithm for different values of β and to calculate the curve which gives us the area of PV modules A_{PV} as a function of this angle:

$$A_{PV}^\beta(\beta) \tag{25}$$

(3) Calculating the maximum β^* , in the curve which represents the total energy:

$$E_{PV}^\beta(\beta) = H_i^\beta(\beta) \cdot A_{PV}^\beta(\beta) \tag{26}$$

4. Results and discussions

The aim of this section is to estimate the effect of the non-ideal position of the PV modules on the annual energy and the distribution of PV modules on flat roofs. This evaluation indicators are analysed for several geographic locations.

4.1. Case study

Gernaat et al. [53] estimate that a global roof area of 113 billion (m²) with 36 billion (m²) will potentially be suitable for rooftop PV systems. The northern hemisphere approximately holds 90% of the World Population [54]. In addition, as the roofs of buildings are a good location for the energy production, the northern hemisphere is the hemisphere that has the most roof surface. For example, the total floor area of residential buildings amounts around 19 billion (m²) in the European Union [55]. Single family houses represent two thirds of the residential floor space. These are the reasons for focusing the study on the northern hemisphere.

The SolarGIS software [56] is a map-based online simulation software with local geographical data of high accuracy and a spatial resolution to the site specifications. Fig. 8 shows a map of the global horizontal solar irradiation for all over world. From this map can be obtained the following conclusions for the northern hemisphere: (i) In the places located between latitudes 15°N and 35°N, it is received the greatest amount of solar irradiance. Approximately, 90% of the solar irradiance gets the Earth surface as beam solar irradiance. This work studies cities in countries such as Mexico, Pakistan, and Egypt; (ii) The next favourable belt lies between latitudes 0°N and 15°N. This work studies cities in countries such as Colombia, and Thailand; (iii) In the places located between latitudes 35°N and 45°N, there are significant seasonal variations, therefore these areas receive less solar irradiance. This work studies cities in countries of these areas such as Spain, and

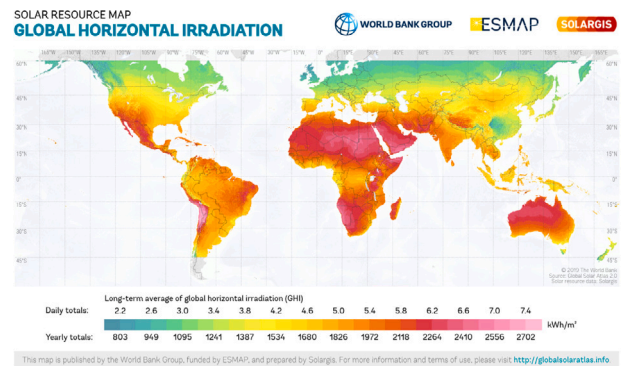


Fig. 8. Global horizontal irradiation map for all over world [56].

Table 2
Cities under study.

	Cities	Latitude	Longitude	Altitude
1	Medellin (Colombia)	06°14'38"N	75°34'04"W	1469 (m)
2	Bangkok (Thailand)	13°45'14"N	100°29'34"E	9 (m)
3	Morelia (Mexico)	19°42'10"N	101°11'24"W	1921 (m)
4	Karachi (Pakistan)	24°52'01"N	67°01'51"E	14 (m)
5	Cairo (Egypt)	30°29'24"N	31°14'38"W	41 (m)
6	Almeria (Spain)	36°50'07"N	02°24'08"W	22 (m)
7	Toronto (Canada)	43°39'14"N	79°23'13"W	106 (m)
8	Wien (Austria)	48°15'00"N	16°21'00"E	203 (m)
9	Hamburg (Germany)	53°33'00"N	10°00'03"E	19 (m)
10	Helsinki (Finland)	60°10'10"N	24°56'07"E	23 (m)

Canada; (iv) The areas located beyond 45°N receive the smaller amount of solar irradiance. Approximately half of the solar irradiance gets the Earth surface as diffuse solar irradiance due to the frequent cloud cover. This work studies cities in countries such as Austria, Germany and Finland which are located in these areas.

In order to generate a complete image of the variation all over the World of the evaluation indicators, this study is focused on 10 cities that cover latitudes from 6 (°) to 60 (°) in the northern hemisphere with a step of 6 (°), approximately. All the cities that have been chosen are located in different climatic areas and their latitudes are different enough to allow a deep analysis. Table 2 shows the geographic characteristics of the cities under study.

Table 3
Optimum tilt angle and maximum annual solar irradiation.

City	Jacobson's formula		Proposed method	
	β_{opt} (°)	Maximum annual irradiation (MWh/m ²)	β_{opt} (°)	Maximum annual irradiation (MWh/m ²)
Medellin (Colombia)	8.3	1.8274	4.5	1.8299
Bangkok (Thailand)	15.3	1.8843	13.2	1.8852
Morelia (Mexico)	20.0	2.1772	19.9	2.1772
Karachi (Pakistan)	23.5	2.2398	23.6	2.2398
Cairo (Egypt)	26.6	2.2764	24.2	2.2779
Almeria (Spain)	30.0	2.1084	30.3	2.1084
Toronto (Canada)	33.0	1.4442	30.6	1.4450
Wien (Austria)	34.8	1.3397	32.9	1.3408
Hamburg (Germany)	36.7	1.1700	36.8	1.1701
Helsinki (Finland)	39.0	1.0558	38.6	1.0562

4.2. Results of tilt angle and annual energy in ideal position

Based on the method previously described, we calculate the ideal position of a *PV* module with the effect of the weather conditions. The contributions of each type of solar irradiance are calculated using the equations presented in Section 2 for different locations.

A MATLAB code calculates the direct, diffuse, and reflected components of the solar irradiance. The MATLAB code uses the satellite-derived *PVGIS* data [57] for each city under study as inputs of monthly-averaged beam and diffuse solar irradiation. The effect of the weather conditions is taken into account with the method proposed by [42].

The validation of the proposed method is done using Jacobson's formula [31] (see Table 1). The Jacobson's formula is considered a good fit for real-life *PV* systems [58], and it has widely been used [33,59,60]. Table 3 shows the optimum tilt angle and the adjusted annual solar irradiation which gets a tilted surface in the ideal position $\mathbb{H}^a(\beta_{opt}, 0)$, for these 10 cities, using the Jacobson's formula and the proposed method. As shown in this table, the adjusted annual solar irradiation obtained with both models are very similar. Therefore, the proposed model is considered to be validated as the deviations are not greater than 0.30%.

4.3. Influence of the non-ideal position on energy loss

The graphs that make it possible to analyse the energy losses have been generated with the (7) previously described, the *PVGIS* data [57] and the method proposed by [42]. Fig. 9 shows the energy loss for the cities that have been studied. The algorithm running time is about 97 (s) to examine a fixed azimuth angle and all possible tilt angles between 0 and 90 (°) in one-degree steps in order to calculate the annual solar irradiation on a personal computer equipped with Windows 10, 64 Bits, processor Intel Core i5-9500 3.00 Ghz, and 16 GB of RAM.

Our calculations show that the installation of *PV* modules with $\gamma = 0$ (°) and tilt angle deviations of up to 10 (°) in relation to the optimum tilt angle has a very little influence on the incoming solar irradiation of up to 1%. This is true in all the cities that have been studied. If the tilt angle deviations are increased, their influence on the incoming solar irradiation becomes stronger: tilt angle deviations of 21 to 23 (°) produce 5% energy losses, tilt angle deviations of 31 to 33 (°) produce 10% energy losses, tilt angle deviations of 37 to 40 (°) produce 15% energy losses and tilt angle deviations of 43 to 47 (°) produce 20% energy losses. Therefore, in Medellin, a tilt angle of 5 (°), which is the minimum tilt angle necessary to allow the natural cleaning action of rainfall [36] can be used.

Furthermore, our calculations show that the installation of *PV* modules with the optimum tilt angle and azimuth angle deviations in relation to the $\gamma = 0$ (°) has a very little influence in a city located in a lower latitude. In Medellin, azimuth angle deviations of up to 90 (°) in relation to the optimum azimuth angle have a very little influence on

the incoming solar irradiation of up to 1%. As the latitude of the city gets higher, there is a decrease of the azimuth angle on the incoming solar irradiation of up to 1%. In Helsinki, azimuth angle deviations of up to 23 (°) in relation to the optimum azimuth angle have a very little influence on the incoming solar irradiation of up to 1%. In the other hand, when the azimuth angle deviations increase, the influence on the incoming solar irradiation becomes stronger: azimuth angle deviations of 48 (°) produce 5% energy losses, azimuth angle deviations of 69 (°) produce 10% energy losses. Therefore, the influence of the tilt angle is greater than the influence of the azimuth angle.

In order to get an explanation for these results, various factors should be contemplated. Firstly, it is well known that the higher the latitude is the greater the difference between the summer and the winter irradiance would be for these places. Therefore, as the latitude increases, the tilt angle should progressively give priority to the summer collection over the winter collection. Therefore, the optimum tilt angle tends to be larger when the latitude is higher. Secondly, the higher the latitude is the greater the curvature in relation to the tilt angle and also greater the energy loss would be, as it is shown in Fig. 9. That means that the energy losses due to tilt angle deviations are greater as the latitude increases. Furthermore, it is necessary to remember that, with the method we have presented, the distribution of annual solar irradiance is specific for each particular site, with remarkable variations produced by the distribution of the local cloudy cover. Therefore, it is difficult to get more general conclusions related to the tilt angle. Eventually, the azimuth angle influence on energy loss is always very little although it becomes a bit bigger when the latitude increases. In conclusion, it is crucial to pay more attention to how to properly choose the angles in sites located in high latitude zones.

4.4. Influence of the non-ideal tilt on distribution of *PV* modules on flat roofs

This section shows the results obtained with the packing algorithm described in Section 3.2. The optimization algorithm has been implemented with the commercial software Mathematica™. Just for this presentation, the city of Almeria (Spain), with latitude 36°50'07"N, longitude 02°24'08"W and altitude 22 (m) has been chosen.

Taking into account the Spanish Government Technical Report [11], for the specific location of Almeria (Spain) the value of θ_{10} (13) of the standard on December 21 at 10 : 00 is 63.4 (°). Next, the influence of the standard [11] for this particular location is analysed. Fig. 10 shows three curves. Firstly, the black curve represents the dawn and the sunset hours of each day through the year. Secondly, by using the (4), the hours of each day through which the cosine of the incident angle is positive have been calculated in order to ensure that the Sun faces towards the surface. These values are represented with the red curve. Eventually, by means of (13) the hours (for each day of the year) in which it is fulfilled that $\theta_{10} = 63.4$ (°) have been calculated and then they have been represented with the blue curve. In between these curves of the graph the absence of shading between the *PV* modules is

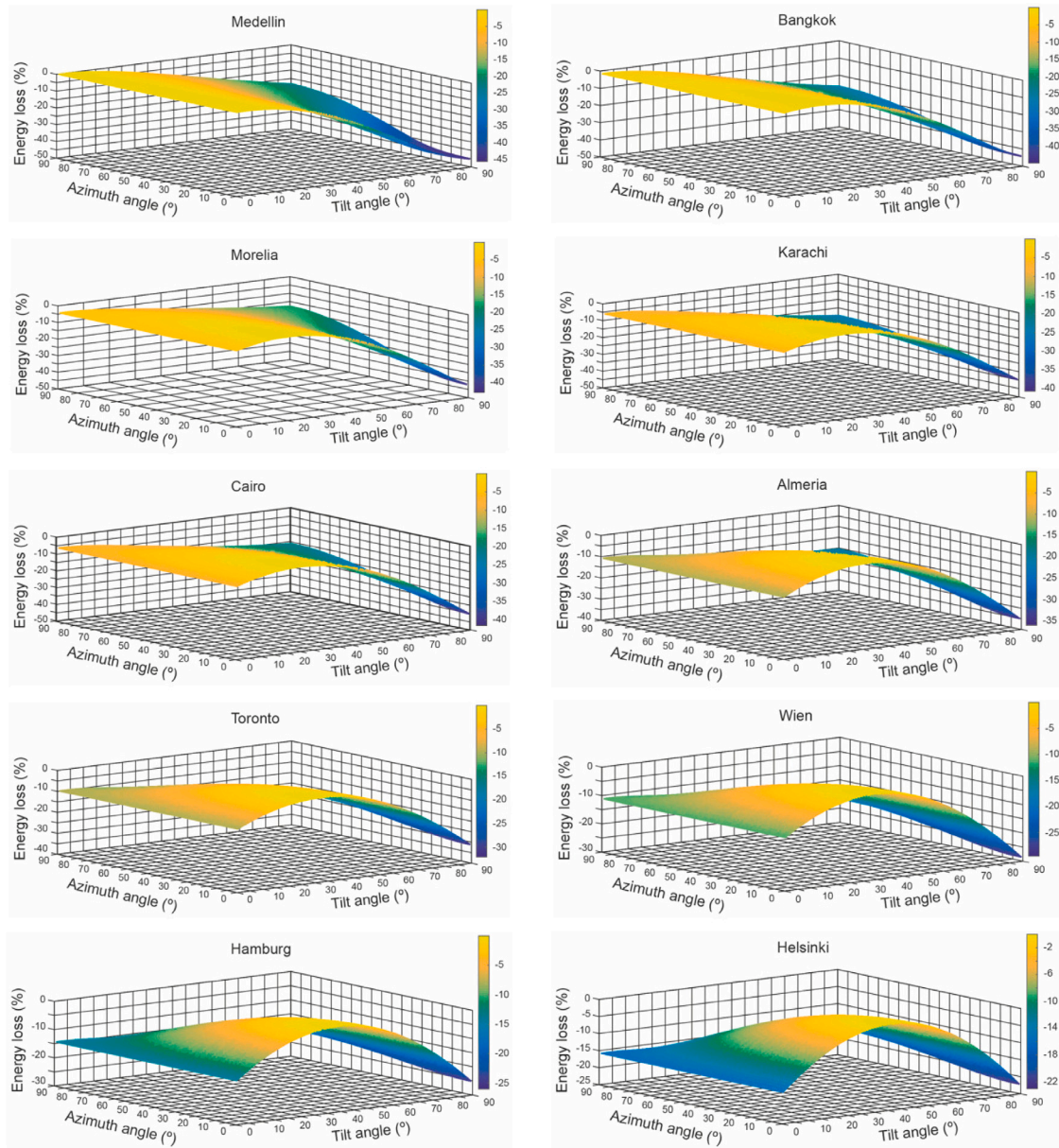


Fig. 9. Energy loss for the cities under study.

guaranteed. This graph shows that black curve and blue curve are the same curve when the declination δ is positive. This happens in the case of the selected location between the 80th and the 267th days.

$[T_1(n), T_2(n)]$ are named operating hours of the PV system, they are hours through which the absence of shading is guaranteed and simultaneously the $\cos \theta_i \geq 0$. Therefore, the planning to calculate the adjusted solar irradiation on a tilted surface, $\mathbb{H}_t(n, \beta, \gamma)$ is going to be modified. Basing on the (1), the adjusted hourly distribution of solar irradiance on a tilted surface, $\mathbb{I}_t(n, T, \beta, \gamma)$ (W/m^2) has been integrated between $T_1(h)$ and $T_2(h)$ [20]:

$$\mathbb{H}_t(n, \beta, \gamma) = \int_{T_1(n)}^{T_2(n)} \mathbb{I}_t(n, T, \beta, \gamma) dT \quad (27)$$

With a discretization of 1° the integral for each one of the values of the interval $[0, 90]$ has been computed [20]:

$$\mathbb{H}_t^\beta(\beta) = \int_1^{365} \mathbb{H}_t(n, \beta, 0) dn \quad (28)$$

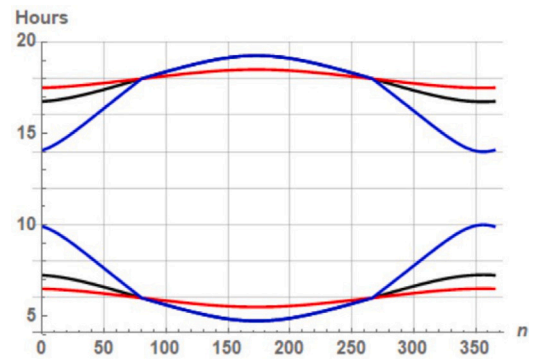


Fig. 10. Operating hours of the PV system with no shading.

The Fig. 11 contains the plot of $\mathbb{H}_t^\beta(\beta)$ against β . It can be noticed that, when the (27), which allows to ensure the absence of shades in between

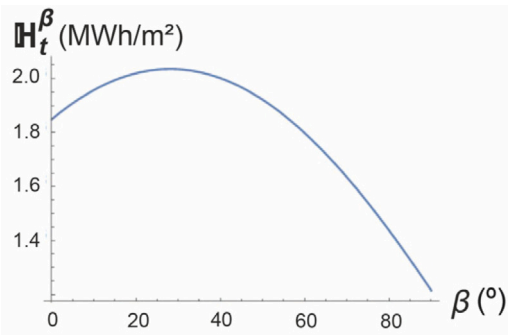


Fig. 11. Variation of $H_t^\beta(\beta)$ with tilt angle β .

the PV modules, is used then there is a maximum in $\beta_{opt} = 28^\circ$ and the optimum total irradiation during a year is 2.03608 (MW h/m²). These values can be compared to those shown in Table 3, where the effect of shading had not been considered.

Eventually, the solution of the packing algorithm is going to be presented. This algorithm enables to deal with any shape and any orientation of the roof. As an example of this, in Fig. 12 a case where the dimensions of the terrace T are given by its five vertices (in clockwise direction) is shown:

$$(-b, 0), (0, 0), (0, -a), (-b/2, -a), (-b, -b/2) \quad (29)$$

where $a = 24$ (m) and $b = 12$ (m). The angle that the terrace forms with the North–South direction is supposed to be $\alpha = 30^\circ$. Without any loss of generalization, they can be taken $e_t = 0.025$ (m), $e_l^m = 1$ (m) and $e_b = 1$ (m) just for maintenance, cleaning and installation works. With regard to the spacing that the standard e_l^{st} imposes, its value which is given by (14), will depend on the selected tilt β .

With regard to the type of PV module it has been chosen, without any loss of generalization, the model JAM72S20 440–465/MR manufactured by JA Solar, with a rated maximum power of 450 (W) and dimensions of 2120 × 1052 (mm). It is important to highlight that the algorithm considers four possible rack configurations: 1V, 1H, 2V and 2H, rejecting rack configurations 3H and 3V due to the excessive height that the system reaches. In this nomenclature it is considered that: (i) numbers 1,2,3,... represent the number of rows of PV modules that have been used; (ii) V stands for the rack configuration in which L is the reference to the tilt angle and H stands for the rack configuration in which the magnitude W is the reference to the tilt angle.

The algorithm gets, by using the packing scheme, the orientation, the rack configuration, the position and the number of PV modules which maximizes the total area of PV modules, A_{PV} . The brute force algorithm evaluates all the possibilities. As the optimum tilt for this location is $\beta_{opt} = 30.3^\circ$, all the tilt values between $[0, 60]$ ($^\circ$) have been considered with steps of 1 ($^\circ$). Just for this example the algorithm running time is about 54 (s) on a personal computer (Intel Core™ i5-1035G1 CPU, 1.00 GHz), showing its capacity to solve problems with a much bigger dimension.

As an example of how the algorithm runs, the best solution of the packing scheme with $\beta_{opt} = 30^\circ$, for the particular case that has been considered is shown in Fig. 11. The best solution consists of 33 PV modules with the rack configuration 1V, with a maximum area of $A_{PV} = 73.59$ (m²). The spacing e_l , get with (15), is 2.11 (m), a value that has been imposed by the standard e_l^{st} , due to the shading produced by PV modules in a vertical position.

For β_{opt} it is clear that the solar irradiation captured by the PV module is the maximum one. But, once $\beta \in [0, 60]$ ($^\circ$) has been swept, the maximum value for the area of PV modules A_{PV} as a function of the mentioned angle $A_{PV}^\beta(\beta)$ is known. Fig. 13 shows how it is possible to remarkably increase the area of PV modules by decreasing the tilt

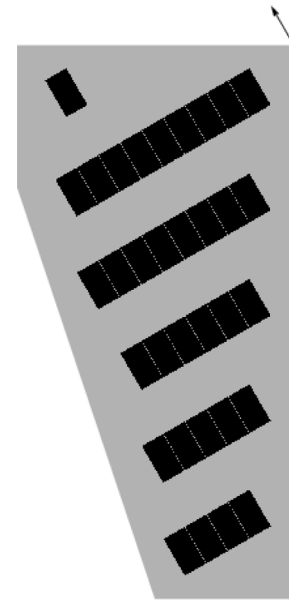


Fig. 12. Optimal solution for A_{PV} with $\beta_{opt} = 30.3^\circ$.

β in relation to β_{opt} , thanks to the reduction in the spacing imposed by the standard e_l^{st} . For each value of tilt β , definitely a different configuration with regard to its orientation, its position and its number of PV modules is obtained.

Eventually, the energy curve $E_{PV}^\beta(\beta)$, product of $H_t^\beta(\beta)$ and $A_{PV}^\beta(\beta)$ curves, is shown in Fig. 13. The maximum value of the curve in Fig. 13, and therefore, the optimum value of tilt for the PV modules in order to maximize the energy captured by all the PV modules of the roof is $\beta^* = 14^\circ$, getting an energy amount of 186.247 (MW h). If it is compared to the amount of energy obtained with $\beta_{opt} = 30.3^\circ$ which is 149.787 (MW h) it will be confirmed that an increase of 24.34% in the amount of energy can be obtained. It is worth attention that this is a great improvement. This remarkable result shows how important it is to know the solar irradiation not only for the optimum tilt but also for non-ideal positions.

The best solution of the packing scheme for $\beta^* = 14^\circ$, is shown in Fig. 14. The solution in this case consists of 42 PV modules with the rack configuration 1V, with a maximum area of $A_{PV} = 93.67$ (m²) which is much bigger than that of 73.59 (m²) obtained with the packing shown in Fig. 12. The spacing e_l is now only of 1.02 (m), a value which is much smaller than that of 2.11 (m) obtained with $\beta_{opt} = 30.3^\circ$. It is so on account of the smaller shading produced by the PV modules and of the smaller value imposed by the standard e_l^{st} , being even though fulfilled the maintenance value of 1 (m).

Many other simulations varying the dimensions and the shape of the roof and the angle that the terrace forms with the North–South direction have been carried out. These simulations have shown that the best solution has not always an unique orientation and that the fact of decreasing or increasing the tilt of the PV module is not always worth doing. For each particular case the packing algorithm should be used together with the calculation of the non-ideal annual irradiation to get the best solution.

5. Conclusions

This paper analyses in detail the energy losses and the distribution of the photovoltaic modules on flat roofs of the photovoltaic systems in non-ideal positions for urban applications. This engineering problem is highly complex as it involves 10 variables: the available flat roof area, the shape and the orientation of the available flat roof area, the

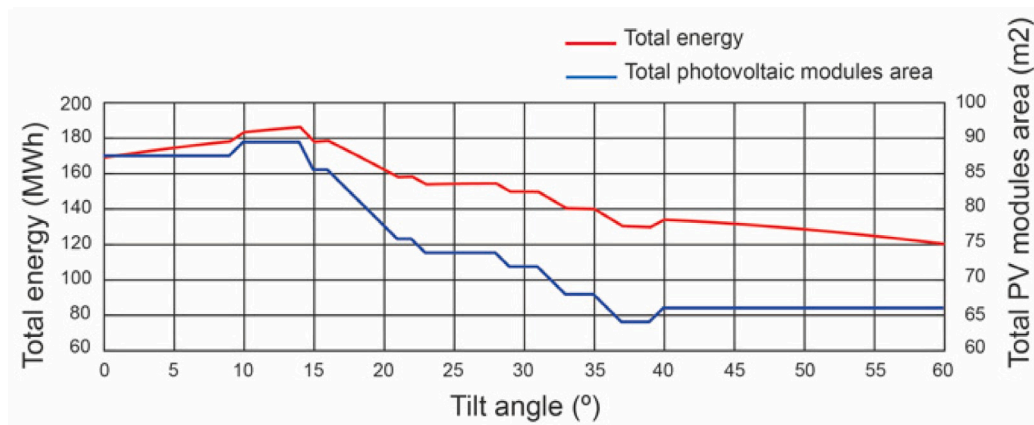


Fig. 13. Energy and PV panels' area as function of the tilt.

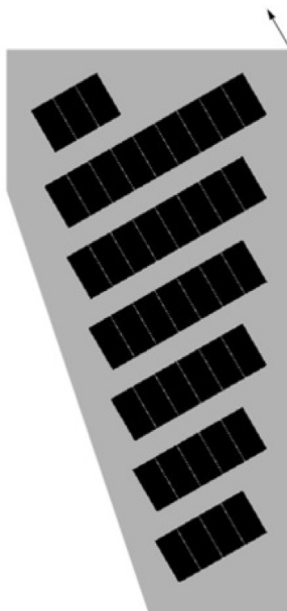


Fig. 14. Optimal solution for A_{PV} with $\beta^* = 14^\circ$.

dimensions (length and width) of the commercial photovoltaic module, the orientation and the position of the photovoltaic modules, the number of the photovoltaic modules, the minimum distances (maintenance operations, to avoid shading effects) between rows of photovoltaic modules and the minimum distance to the terrace boundary. In this context, this paper aims to present a study to assist the decision-making. The study was carried out for 10 cities of the World in the northern hemisphere for all the possible tilts and orientations of the photovoltaic systems. The annual solar irradiation incident on a photovoltaic system in non-ideal positions for urban applications have been determined using the mathematical model presented in the section about governing equations by developing a *MATLAB* code. The ideal position of the photovoltaic systems has also been determined by the application of Cavalieri's principle. Two evaluation indicators are proposed to study the photovoltaic systems in non-ideal positions the energy loss and the distribution of the photovoltaic modules on flat roofs.

The following conclusions have been drawn:

(i) The results demonstrate that non-ideal tilt and azimuth angles can also lead to acceptable levels of electric energy generation, but it is necessary to assess the degree of energy reduction that these non-ideal positions produce.

(ii) A photovoltaic system installed with orientation 0° and tilt angle deviations of up to 10° in relation to the optimum tilt angle has a very little influence on the energy losses. This is true in all the cities that have been studied.

(iii) With orientation 0° and an increase of the tilt angle deviations, the influence on the incoming solar irradiation is stronger: 5% energy losses with deviations of the tilt angle between 21 and 23° , 10% energy losses with deviations of the tilt angle between 31 and 33° , 15% energy losses with deviations of the tilt angle between 37 and 40° and 20% energy losses with deviations of the tilt angle between 43 and 47° .

(iv) The orientation of a photovoltaic system has a lower influence on energy losses than the optimal inclination of the photovoltaic system.

With regard to the impact of the distribution of photovoltaic modules on the flat roofs, it has been found that the option of non-orientating the photovoltaic modules on its β_{opt} , sometimes is very advantageous. In the proposed example we have obtained a 24.3% more total energy captured by the photovoltaic system. The aim is to get the biggest area of energy generation of the photovoltaic system which compensates for the diminution in the solar irradiance captured by each of the photovoltaic modules.

These analysis enables to find the optimal answer to the following practical questions: what number of photovoltaic modules is required?, which is the right position of the photovoltaic module?, and what orientation of photovoltaic modules is right one?. There are many installers of photovoltaic systems who would benefit from studies about this issue.

CRediT authorship contribution statement

A. Barbón: Conceptualization, Methodology. **C. Bayón-Cueli:** Software, Methodology, Writing – original draft. **L. Bayón:** Conceptualization, Methodology. **C. Rodríguez-Suanzes:** Software, Conceptualization, Methodology.

Declaration of competing interest

The authors declare that they have no known competing financial interests or personal relationships that could have appeared to influence the work reported in this paper.

Acknowledgement

We wish to thank Gonvarri Solar Steel [61] for his contribution in this paper.

References

- [1] UN. World urbanization prospects: revision 2014. United Nations; 2014.
- [2] Eurobserv' ER. Solar thermal and concentrated solar power barometer. 2019, Available from: <https://www.eurobserv-er.org/solar-thermal-and-concentrated-solar-power-barometer-2018/>. [Accessed on: 6 March 2021].
- [3] Jacobson MZ, Delucchi MA, Bauer ZAF, Goodman SC, Chapman WE, Cameron MA, Bozonnat C, Chobadi L, Clonts HA, Enevoldsen P, Erwin JR, Fobi SN, Goldstrom OK, Hennessy EM, Liu J, Lo J, Meyer CB, Morris SB, Moy KR, O'Neill PL, Petkov I, Redfern S, Schucker R, Sontag MA, Wang J, Weiner E, Yachanin AS. 100% clean and renewable wind, water, and sunlight (WWS) all-sector energy roadmaps for 139 countries of the world. *Joule* 2017;1:108–21, (Alphabetical).
- [4] Yadav S, Panda SK, Hachem-Vermette C. Method to improve performance of building integrated photovoltaic thermal system having optimum tilt and facing directions. *Appl Energy* 2020;266:114881.
- [5] López-Escalante MC, Navarete-Astorga E, Perez MGabás, Ramos-Barrado JR. Photovoltaic modules designed for architectural integration without negative performance consequences. *Appl Energy* 2020;279:115741.
- [6] Sánchez-Pantoja N, Vidal R, Pastor MC. Aesthetic impact of solar energy systems. *Renew Sustain Energy Rev* 2018;98:227–38.
- [7] Sánchez-Pantoja N, Vidal R, Pastor MC. Aesthetic perception of photovoltaic integration within new proposals for ecological architecture. *Sustainable Cities Soc* 2018;39:203–14.
- [8] Scognamiglio A. 'Photovoltaic landscapes': Design and assessment. a critical review for a new transdisciplinary design vision. *Renew. Sustain. Energy Rev.* 2016;55:629–61.
- [9] Yang Y, Campana PE, Stridh B, Yan J. Potential analysis of roof-mounted solar photovoltaics in Sweden. *Appl Energy* 2020;279:115786.
- [10] Romero Rodríguez L, Duminiel E, Sánchez Ramos J, Eicker U. Assessment of the photovoltaic potential at urban level based on 3D city models: A case study and new methodological approach. *Sol Energy* 2017;146:264–75.
- [11] IDAE. Technical conditions for pv installations connected to the grid [in spanish]. Spanish Government Technical Report. Report Available from the Publication Services of the Institute for Diversification and Energy Savings, Spain, 2011, Available from: <http://www.idae.es> [Accessed on: 6 March 2021].
- [12] Byrne J, Taminiau J, Kurdgelashvili L, Nam Kim K. A review of the solar city concept and methods to assess rooftop solar electric potential, with an illustrative application to the city of seoul. *Renew Sustain Energy Rev* 2015;41:830–44.
- [13] Md Mahamudul Hasan Mithhu, Ahmed Rima T, M. Ryyan Khan. Global analysis of optimal cleaning cycle and profit of soiling affected solar panels. *Appl Energy* 2021;285:116436.
- [14] Gupta V, Sharma M, Kumar Pachauria R, Dinesh Babu KN. Comprehensive review on effect of dust on solar photovoltaic system and mitigation techniques. *Sol Energy* 2019;191:596–622.
- [15] Bahrami A, Onyeka Okoye C, Atikol U. Technical and economic assessment of fixed, single and dual-axis tracking PV panels in low latitude countries. *Renew Energy* 2017;113:563–79.
- [16] Nsengiyumva W, Guo Chen S, Hu L, Chen X. Recent advancements and challenges in solar tracking systems (STS): A review. *Renew Sustain Energy Rev* 2018;81:250–79.
- [17] Gonvarri Solar Steel. 2021, Available from: <https://www.gsolarsteel.com/>. [Accessed on: 19 May 2021].
- [18] Tomson T. Discrete two-positional tracking of solar collectors. *Renew Energy* 2008;33:400–5.
- [19] Mousazadeh H, Keyhani A, Javadi A, Mobli H. A review of principle and sun-tracking methods for maximizing solar systems output. *Renew Sustain Energy Rev* 2009;13:1800–18.
- [20] Duffie JA, Beckman WA. Solar engineering of thermal processes. John Wiley & Sons; 2013.
- [21] Lv Y, Si P, Rong X, Yan J, Feng Y, Zhu X. Determination of optimum tilt angle and orientation for solar collectors based on effective solar heat collection. *Appl Energy* 2018;219:11–9.
- [22] Chinchilla M, Santos-Martín D, Carpintero-Rentería M, Lemon S. Worldwide annual optimum tilt angle model for solar collectors and photovoltaic systems in the absence of site meteorological data. *Appl Energy* 2021;281:116056.
- [23] Amaro de Silva R, Brito MC. Spatio-temporal PV forecasting sensitivity to modules' tilt and orientation. *Appl Energy* 2019;255:113807.
- [24] Hafez AZ, Soliman A, El-Metwally KA, Ismail IM. Tilt and azimuth angles in solar energy applications – a review. *Renew Sustain Energy Rev* 2017;77:147–68.
- [25] Heywood H. Operating experience with solar water heating. *J Instit Heat Ventil Energy* 1971;39:63–9.
- [26] Lunde PJ. Solar thermal engineering: space heating and hot water systems. John Wiley & Sons; 1980.
- [27] Chinnery DNW. Solar Water Heating in South Africa. National Building Research Institute (South Africa), CSIR Report, 44, 1971, p. 248.
- [28] Luque A, Hegedus S. Handbook of photovoltaic science and engineering. John Wiley & Sons; 2003.
- [29] Chang TP. The Sun's apparent position and the optimal tilt angle of a solar collector in the northern hemisphere. *Sol Energy* 2009;83:1274–84.
- [30] Talebizadeh P, Mehrabian MA, Abdolzadeh M. Determination of optimum slope angles of solar collectors based on new correlations. *Energy Sources A* 2011;33:1567–80.
- [31] Jacobson MZ, Jadhav V. World estimates of PV optimal tilt angles and ratios of sunlight incident upon tilted and tracked PV panels relative to horizontal panels. *Sol Energy* 2018;169:55–66.
- [32] Chen XM, Li Y, Zhao BY, Wang RZ. Are the optimum angles of photovoltaic systems so important? *Renew Sustain Energy Rev* 2020;124:109791.
- [33] Al Garni HZ, Awasthi A, Wright D. Optimal orientation angles for maximizing energy yield for solar PV in Saudi Arabia. *Renew Energy* 2019;133:538–50.
- [34] Sánchez E, Izard J. Performance of photovoltaics in non-optimal orientations: an experimental study. *Energy Building* 2015;87:211–9.
- [35] Barbón A, Barbón N, Bayón L, Sánchez-Rodríguez JA. Optimization of the distribution of small scale linear fresnel reflectors on roofs of urban buildings. *Appl Math Model* 2018;59:233–50.
- [36] Portolan dos Santos I, Rüther R. Limitations in solar module azimuth and tilt angles in building integrated photovoltaics at low latitude tropical sites in Brazil. *Renew Energy* 2014;63:116–24.
- [37] Liu BYH, Jordan RC. The long-term average performance of flat-plate solar energy collectors. *Sol Energy* 1963;7:53–74.
- [38] Danandeh MA, Mousavi GSM. Solar irradiance estimation models and optimum tilt angle approaches: A comparative study. *Renew Sustain Energy Rev* 2018;92:319–30.
- [39] Antonanzas-Torres F, Urraca R, J. Polo J, Perpiñán Lamigueiro O, Escobar R. Clear sky solar irradiance models: A review of seventy models. *Renew Sustain Energy Rev* 2019;107:374–87.
- [40] Salazar G, Gueymard C, Bezerra Galdino J, Castro Vilela O. Solar irradiance time series derived from high-quality measurements, satellite-based models, and reanalyses at a near-equatorial site in Brazil. *Renew Sustain Energy Rev* 2020;117:109478.
- [41] Fan J, Chen B, Wu L, Zhang F, Lu X. Evaluation and development of temperature-based empirical models for estimating daily global solar radiation in humid regions. *Energy* 2018;144:903–14.
- [42] Barbón A, Fortuny Ayuso P, Bayón L, Fernández-Rubiera JA. Predicting beam and diffuse horizontal irradiance using Fourier expansions. *Renew Energy* 2020;154:46–57.
- [43] Hottel HC. A simple model for estimating the transmittance of direct solar radiation through clear atmosphere. *Sol Energy* 1976;18:129–34.
- [44] Liu BYH, Jordan RC. The interrelationship and characteristic distribution of direct, diffuse and total solar radiation. *Sol Energy* 1960;4(3):1–19.
- [45] WRDC. World radiation data Centre. 2020, Available from: <http://wrdc.mgo.rssi.ru/>. [Accessed on: 6 March 2021].
- [46] Moore DS, Notz WI, Flinger MA. The basic practice of statistics. W. H. Freeman; 2013.
- [47] Bayón-Cueli C, Barbón A, Bayón L, Barbón N. A cost-energy based methodology for small-scale linear fresnel reflectors on flat roofs of urban buildings. *Renew Energy* 2020;146:944–59.
- [48] Barbón A, Bayón-Cueli C, Bayón L, Fortuny Ayuso P. Influence of solar tracking error on the performance of a small-scale linear fresnel reflector. *Renew Energy* 2020;162:43–54.
- [49] Barbón A, Fernández-Rubiera JA, Martí nez Valledor L, Pérez-Fernández A, Bayón L. Design and construction of a solar tracking system for small-scale linear Fresnel reflector with three movements. *Appl Energy* 2021;285:116477.
- [50] Shukla KN, Rangnekar S, Sudhakar K. Comparative study of isotropic and anisotropic sky models to estimate solar radiation incident on tilted surface: A case study for Bhopal, India. *Energy Rep* 2015;1:96–103.
- [51] Mehleri ED, Zervas PL, Sarimveis H, Palyvos JA, Markatos NC. Determination of the optimal tilt angle and orientation for solar photovoltaic arrays. *Renew Energy* 2010;35:2468–75.
- [52] Spivak M. Calculus. 2008, Michael Spivak.
- [53] Gernaat DEHJ, Sytze de Boer H, Dammeier LC, van Vuuren DP. The role of residential rooftop photovoltaic in long-term energy and climate scenarios. *Appl Energy* 2020;115705.
- [54] UN. World population prospects 2019. United nations. 2019, Available from: <https://population.un.org/wpp/> [Accessed on: 6 March 2021].
- [55] Odyssee-Mure. Energy efficiency trends in buildings in the EU lessons from the ODYSSEE MURE project. 2015, Available from: <http://www.odyssee-mure.eu/publications/br/energy-efficiency-trends-policies-buildings.pdf>, [Accessed on: 6 March 2021].
- [56] SOLARGIS. Available from: <https://solargis.com/maps-and-gis-data/download/world/>. [Accessed on: 6 March 2021].
- [57] PVGIS. Joint research centre (jrc). 2020, Available from: http://re.jrc.ec.europa.eu/pvg_tools/en/tools.html#PVP. [Accessed on: 6 March 2021].

- [58] Müller J, Folini D, Wild M, Pfenninger S. CMIP-5 models project photovoltaics are a no-regrets investment in Europe irrespective of climate change. *Energy* 2019;171:135–48.
- [59] Ascencio-Vásquez J, Brecl K, Topič M. Methodology of Köppen-Geiger-Photovoltaic climate classification and implications to worldwide mapping of PV system performance. *Sol Energy* 2019;191:672–85.
- [60] Tröndle T, Pfenninger S, Lilliestam J. Home-made or imported: On the possibility for renewable electricity autarky on all scales in Europe. *Energy Strategy Rev* 2019;26:100388.
- [61] Gonvarri Solar Steel. Available from: <https://www.gsolarsteel.com/>. [Accessed on: 23 June].